Superparamagnetic anisotropic elastomer connectors exhibiting reversible magneto-piezoresistivity.

*José L. Mietta[1], Guillermo Jorge[2], Oscar E. Perez[3], Thomas Maeder[4], R. Martín Negri[1]**

1. Instituto de Química Física de Materiales, Ambiente y Energía (INQUIMAE). Departamento de Química Inorgánica, Analítica y Química Física. Facultad de Ciencias Exactas y Naturales. Universidad de Buenos Aires.

2. Departamento de Física. Facultad de Ciencias Exactas y Naturales. Universidad de Buenos Aires.

3. Departamento de Industrias. Facultad de Ciencias Exactas y Naturales. Universidad de Buenos Aires.

4. Laboratoire de Production Microtechnique, (LPM). École Polytechnique Fédérale de Lausanne (EPFL), Lausanne, Switzerland.

* To whom correspondence should be addressed:

Ciudad Universitaria, Pabellón II. INQUIMAE. C1428EGA, Buenos Aires, Argentina.

e-mail: rmn@qi.fcen.uba.ar TE: xx54-11-4576-3358 FAX: xx54-11-4576-3341

Abstract

An anisotropic magnetorheological composite formed by dispersions of silver-covered magnetite microparticles (Fe_3O_4@Ag) in polydimethylsiloxane (PDMS) displaying electrical conduction only in one preferred direction is presented. A set-up for applying and detecting electrical conduction through the composite is described and applied to characterize the behavior of the system in on-off commutation cycles. The composite is obtained by loading the polymer with relatively low concentration of fillers (5% *w/w* of the total weight) and curing it in the presence of a uniform magnetic field. The fillers appear in the final composite as an array of needles, i.e. pseudo-chains of particles aligned in the direction of the magnetic field. Using Fe_3O_4 nanoparticles (13 nm) it is possible to obtain cured composites in a superparamagnetic state, that is, without magnetic hysteresis at room temperature. Hysteresis is not found in the elastic properties either; in particular, Mullins effects (change of physical properties after the first strain-stress cycle) were not observed.

No measurable transversal electrical conduction was detected (transversal resistivity larger than 62 MΩ·cm). Thus, significant electrical conductivity is present only between contact points that are exactly facing each other at both sides of the composites in the direction parallel to the needles. The I-V curves in that direction have ohmic behavior and exhibit both piezoresistance and magnetoresistance, that is, the electrical conductivity in the direction parallel to the pseudo-chains increases when a pressure (i.e. compressive stress) is applied at constant magnetic field and/or when a magnetic field is applied at constant pressure. The materials do not exhibit magnetoelectric or piezoresistive hysteresis. These characteristics illustrate the high potentiality of these systems in elastic connectors where electrical conduction can be varied by external mechanical or magnetic forces.

KeyWords: Piezoresistivity, magnetoresistivity, magnetoelastomers

1. Introduction

Magnetorheological (MR) materials are those whose mechanical properties can be modified by externally applied magnetic fields. One type of MR materials are the composites formed by dispersing magnetic filler particles into an elastomer polymeric matrix, referred as magnetorheological elastomers (MRE) [1–3]. A simple procedure to obtain MRE materials is curing the filler-elastomer composite in the presence of a uniform magnetic field (H_{curing}) which induces agglomerations of the filler particles into chain-like structures aligned in the direction of the field [4–11]. These cured composites not only present anisotropic elastic properties but the elastic moduli can be now modified by application of magnetic fields (H). Although the dependence of the Young´s modulus with H in MRE has been investigated in several comprehensive studies [6,7,9], there are two closely-related aspects concerning MRE that have not been systematically explored yet: the dependence of other physical properties with external driving forces has been scarcely reported and the implementation of real devices based on MRE is still in its very beginnings [10,12,13].

In previous work anisotropic MRE using $CoFe_2O_4$ nanoparticles (NPs) and silver-covered Fe_3O_4 microparticles as fillers in polydimethylsiloxane (PDMS) matrixes [14,15] have been characterized. In the present work, an MRE displaying anisotropic piezoresistivity and magnetoresistance effects without transversal electrical conduction (no observed electrical conduction in the direction perpendicular to the pseudo-chains) is presented. Elastic, magnetic, morphological and electrical properties are characterized. Then, the obtained composites are used for implementation of 2-D elastic Zebra-like electrical connectors whose conductivity in commutation cycles is described. A glossary of terms is included in Table 1.

2. Materials and Methods

2.1 Instrumentation

X-ray powder diffraction analysis (XRD) was performed with a Philips X-Pert diffractometer using CuK_α radiation ($\lambda = 0.154056$ nm) and the average size of the Fe_3O_4 crystallites were determined by the Debye-Scherrer equation. The morphology of the Fe_3O_4@Ag-PDMS composite was studied using a scanning electron microscope (SEM) fitted with a field-emission source (FESEM Zeiss Supra 40 Gemini), with the Fe_3O_4 particles also being observed with a Philips EM 301 transmission electron microscope (TEM). A LakeShore 7400 Vibrating Sample Magnetometer (VSM) was used for recording magnetization curves at room temperature. Zero Field Cooling (ZFC) and Field Cooling (FC) magnetization curves were recorded in a Superconducting Quantum Interference Device (SQUID) magnetometer (Quantum Design MPMS XL).

A TEQ 4 (Argentina) potentiostat was used for the voltammetry measurements and the determination of the I-V characteristic curves of the composites.

The analysis of elasticity and the Young´s modulus determination was performed using a Stable Microsystems TA-XT2i Texture Analyzer which compresses the sample (thickness in absence of compression d_i = 3 mm in all cases) at a constant speed (100 μm/s) in the range between 8 to 25% of the initial thickness [15,16]. Specific details of the elastic measurements and data treatment are described in previous work [15,16].

2.2 Synthesis of Fe_3O_4@Ag microparticles

The synthesis method used to prepare silver-covered Fe_3O_4 microparticles was described in detail in a previous article [14]. First, Fe_3O_4 NPs were synthesized by the chemical co-precipitation method where a solution mixture (2:1) of $FeCl_3 \cdot 6H_2O$ and $FeCl_2 \cdot 4H_2O$ in chlorhidric acid was added drop-by-drop to a solution of NaOH (60 °C), under high-speed stirring. The obtained nanocrystals were separated by repeated centrifugation and washing, then dried in a vacuum oven at 40 °C for 24h. The obtained dark brown NPs show a maximum at 13 nm in the log-normal distribution of diameters (determined by TEM images), which is in excellent agreement with the size of the crystallite domains calculated using the Debye-Scherrer relation from XRD, (14 ± 2) nm.

In a second step, the Fe_3O_4 NPs were covered with silver, in order to obtain electrically conductive and superparamagnetic particles. For that, aqueous dispersions of $Ag(NH_3)_2^+$ and Fe_3O_4 NPs in a 10:1 molar ratio were sonicated for 30 min at room temperature. Then the system was heated in a water bath at 50°C for 20 minutes with slow stirring. In the next step, 0.4 M glucose monohydrate solution was added drop-by-drop to the Fe_3O_4-Ag^+ suspension. Stirring was continued for one hour. This synthesis protocol promotes the reduction of Ag (I) ions adsorbed onto Fe_3O_4 particles. These magnetite-silver particles were separated out from the solution by magnetization and then by centrifugation. After the particles were separated, the decanted supernatant liquid was fully transparent. For comparison purposes, silver particles (reddish orange) were produced in a separate batch using the same experimental conditions for each set. For the Fe_3O_4@Ag microparticles the maximum of the diameter distribution is at 1.3 μm (determined by SEM and TEM images).

2.3 Preparation of PDMS-Fe_3O_4@Ag MRE

The magnetic Fe_3O_4 silver-covered microparticles were then used to prepare the textured composite. Briefly, PDMS base and crosslinker agent (Sylgard 184, Dow Corning) were mixed in proportions of 10:1 (*w/w*) at room temperature and then loaded with the magnetic Fe_3O_4 silver-covered microparticles. The amounts of PDMS and fillers were weighed during mixing on an analytical balance, homogenized and placed at room temperature in a vacuum oven for about two hours until the complete absence of any air bubble. Specifically, composite material with 5% *w/w* of Fe_3O_4@Ag was prepared. The still fluid samples were incorporated into a specially designed cylindrical mould (1 cm diameter × *d* thickness, where *d* = 1, 2 or 3 mm) and placed in between the magnetic poles of a Varian Low Impedance Electromagnet (model V3703), which provides highly homogeneous steady magnetic fields. The mould was rotated at 30 rpm to preclude sedimentation, and heated at (75 ± 5) °C in the presence of a uniform magnetic field (0.35 Teslas) during 1 hour to obtain a cured material. Controls without applying the magnetic field were performed. More details are provided in Antonel et al. [15,17] and Mietta et al. [14].

2.4 Piezoresistivity and magnetoresistance of PDMS MRE

A specially designed set-up (Figure 1) was used for measuring the resistivity and piezoresistivity of PDMS-Fe_3O_4@Ag MRE. The device includes two plastic plates, between which the conductive elastomeric material of thickness *d* (*d* = 1, 2 or 3 mm) is placed. Each plastic plate comprises five metal contacts – the conducting regions depicted in Figure 1 - of 1 mm diameter, each one separated from the central contact at a distance of 1.5 mm by a non-conducting region. All the contacts of the top plate match vertically with the contacts of the bottom plate (the plastic plates are kept perfectly

aligned with the use of guide rods). The compressive force was monitored by a sensor, and the voltammetric response was simultaneously recorded using the TQ4 equipment at different pressures. These electrodes allow both measurement of electrical transport through the composite (out of plane, between opposite facing electrodes) and checking the presence of in-plane conductivity (between adjacent electrodes).

The piezoresistive response is measured by compressing the sample with a controlled-displacement press.

The device for measuring magnetoresistance consists of placing the setup described above between the pole pieces of an electromagnet that generates a uniform magnetic field. A Gaussmeter (Group3 DTM-133 Digital Teslameter) was used to test the intensity of the magnetic field. To measure the electrical resistivity in the MRE samples for different values of H, the current flux through the sample was measured under different intensities of H applying an arbitrary and constant pressure between two copper electrodes (ferromagnetic electrodes must be avoided).

2.5 Verification of non- transverse electrical conduction and on-off commutation cycles.

The measurement set-up described in Section 2.4 also allows checking the presence of absence of transverse electrical conduction, by measuring the resistance between adjacent electrodes rather than facing ones.

A potentiostat (TEQ4, Argentina) was used for the voltammetric and chronoamperometric measurements performed in order to evaluate the response of the elastomer composites to an applied voltage during on-off commutation cycles.

3. Results and discussion

3.1 Properties of the fillers

The particles referred here as Fe_3O_4@Ag are actually microparticles composed by several clusters of magnetic material being covered by silver. The individual clusters inside the microparticles are formed by several NPs of Fe_3O_4. The separation between clusters was estimated to be about 10-15 nm [14]. The magnetic, electric, chemical and morphological properties of both Fe_3O_4 NPs and Fe_3O_4@Ag microparticle powders were characterized in a previous work by applying several techniques: VSM and SQUID (ZFC and FC curves) for magnetic, cyclic voltammetry for the electrical, XRD, UV-Vis, FTIR and EDS for the chemical and XRD, TEM and SEM for the morphological properties [14]. From these studies it was determined that the electrical conductivity of the Fe_3O_4@Ag powder presents ohmic behavior. The powders are in the superparamagnetic state for temperatures T greater than the blocking temperature T_B (T_B = 179 K at H=0). The silver content is about 82 % w/w. The oxygen stoichiometry is the one expected (3:4 Fe-O). The iron oxide core has inverse spinel structure and all the Fe_3O_4 particles are covered with silver.

Therefore, in the next sections, only results concerning the properties of the MRE PDMS composites, but not of the fillers, are presented and discussed.

3.2 MRE PDMS composites

3.2.A. Morphology and magnetic properties.

Slices of the cured composites were held in an ad-hoc sample-holder and cut using a sharp scalpel for obtaining the SEM images and photographs shown in Figure 2. This setup provides slices of equal thickness (3 mm) and similar areas (0.8 cm^2) in all directions. These samples were metalized for obtaining the SEM images.

Curing the composites in the presence of a magnetic field under the conditions and setup described in Section 2.1 led to the self-organization of the filler particles into an array of macroscopic chains appearing observable as needles by the naked eye. Needle formation was observed only with magnetic fillers such as Fe_3O_4@Ag and in case of curing the PDMS in the presence of an applied field. The histograms of the observed needle length and diameter are shown in Figure 3.

About 100 SEM images at several magnifications (from 50× to 6000×) were used to estimate the average dimensions and volume fraction (Φ_v) of the chains. Voltages (EHT) of 5 kV and magnifications of 100× (3300 pixels/cm) and 300× (9800 pixels/cm) were typical conditions for determining the average chain length, while 3 kV and 4000× (40 pixels/μm) were used for obtaining the average chain diameter. The calculated average diameter, apparent length and volume density of chains are 10 μm, 1.3 mm, 9 chains/mm^3. The calculated Φ_v and areal density are approximately 0.1% and 7 chains/mm^2 respectively (note: Φ_v is calculated with the maximum of the size distribution, calculated using about 100 SEM images as indicated before).

The results of the magnetic characterization of the PDMS-Fe_3O_4@Ag structured composite with filler concentration 5% *w/w*, both in parallel direction with respect to the inorganic chains, are presented in Figure 4. The magnetic hysteresis curves at 25 °C are shown in Figure 4a, whereas ZFC-FC magnetization vs. temperature curves at H=0.01 Teslas are presented in Figure 4b. The M_S value in Figure 4a is in excellent agreement with the content of magnetite in the composite [14]. The blocking temperature, T_B, of the MRE composites for different orientations of H with respect to the chains were calculated using the data analysis described in previous work [14,18] from the data shown in Figure 4b and ZFC-FC magnetization vs. temperature curves in perpendicular direction with respect to the inorganic needles (not shown). T_B = 175 K

and T_B = 168 K were obtained for the parallel and perpendicular directions (referred to the chains), respectively. This analysis shows that T_B is always lower when the magnetic field is applied in the direction perpendicular to the needles (for a fixed concentration of particles). This is reasonable because it requires a lower temperature to produce the transition from the blocked to the superparamagnetic state when the magnetic field is applied in the direction perpendicular to the needles, due to a decrease in the dipole-dipole interaction in that configuration.

3.2.B. Elastic properties.

Samples of PDMS-Fe_3O_4 5% w/w and PDMS-Fe_3O_4@Ag 5% w/w cured in the presence of the magnetic field were prepared at least as duplicates in both cases. The inter-sample variation of the recovered Young´s modulus ($E_\perp$ and $E_{/\!/}$) was between 5-3 %. The same samples and others (new batch preparation) were used for measuring the electric response. Elasticity results for a 5% *w/w* composite measured in the direction parallel to the needles are shown in Figure 5. Figure 5a shows the typical behavior of a composite under repeated compression, in pressure versus time curves, in which three cycles of slow-compression and fast decompression are illustrated. It is clear from Figure 5a that the composites display a remarkable elastic behavior (the same magnitude of pressure was required to achieve a 20% strain in consecutive cycles of compression) interpretable as the absence of appreciable Mullins effect [19–21]. This behavior was observed regardless the direction of compression ($/\!/$ or $\perp$ respect to the chains), probably because of the separation (non-adhesion) between the polymer matrix and chains (see Figure 3c).

The rise of the stress-strain curves (compression) is contained in Figure 5a. The complete stress-strain curve (compression followed by decompression both at the same

strain change´s rate; i.e 100 μm/s) is similar to the section shown there since no hysteresis was observed. The aspect of the complete strain-stress curve is similar to that shown in references 14-17 for several magnetorheological composites obtained in our group and for that reason is not included here.

Figure 5b shows the response of a given composite that was compressed up to a maximum strain of 20% with the strain then being kept constant for 10 seconds, observing a very short relaxation time that is in agreement with the elastic behavior of the MRE connector composite. The variation of the sample thickness, d, with the applied pressure, P, was recovered from the strain-stress data and very well fitted by exponential curves ($d(P) = d_i \exp(-P/E)$, where d_i is the initial thickness (d_i = 3 mm) and E the Young's modulus). The correlation coefficients (ρ^2) for the exponential fits of stress-strain curves are about 0.9998 for all the measurements. Also a third-order deformation approximation (Mooney–Rivlin law with five parameters) fits the elastomer micromechanics behavior very well [14,19,20]. The reproducibility of the elastic measurements and of the recovered E values from the exponential fits is very high for a given sample, with intra-sample variability lower than 1.5% after successive determinations (about ten for each sample). This statement holds for measurements in both direction (parallel and perpendicular to the needles). The recovered values of the Young´s modulus of PDMS in the absence of fillers, (690 ± 10) kPa, calculated from both fits (exponential law and Mooney-Rivlin law) are coincident and in agreement with reported values in previous work [22–25]. The Young´s moduli of the composite in both directions, parallel and perpendicular to the needles are referred as $E_{\parallel}$ and $E_{\perp}$, and take values of (900 ± 10) and (780 ± 10) kPa, respectively, which corresponds to an elastic anisotropy of ca. 15%, defined as $(E_{\parallel} - E_{\perp}) / E_{\perp}$.

3.2.C. Piezo and Magneto resistivity

Samples of 1, 2 and 3 mm thickness were tested for analyzing the piezoresistive effects, magnetoresistance properties and the on-off commutation cycles in parallel conduction. Similar qualitative results for the three thicknesses were obtained and the described behaviors are independent of the sample thickness. For evaluation of piezoresistivity, electrical resistivities (in Ω·cm) were measured parallel ($\rho_{/\!/}$) and perpendicular ($\rho_{\perp}$) to the direction of the needles as function of the applied pressure (P) in absence of magnetic field. In all cases the pressure was applied in the vertical direction, i.e. parallel to the particle chains. Cyclic voltammograms, using a scan rate of 50 $mV \cdot s^{-1}$, for PDMS-Fe_3O_4@Ag structured composite with filler concentration 5% *w/w* at room temperature are shown in Figure 6a. The arrow shows the increase of the applied pressure. The variation of $\rho_{/\!/}$ with P is shown in Figure 6b, whereas no measureable transverse (in-plane) conductivity ($\rho_{\perp}$ > 62 MΩ·cm) was detected. These results show that anisotropic conduction was obtained and significant conductivity is obtained only in the direction of the needles ($\rho_{/\!/}$ / $\rho_{\perp}$) >~10^6. Resistivities decrease with increasing pressure (in the range 0-300 kPa) and were well fitted as a function of P by inverse exponential laws. Therefore, the obtained MRE can be used as pressure sensors having additionally the interesting feature of an anisotropic response.

Figure 6c shows the dependence of $\rho_{/\!/}$ with the applied magnetic field. $\rho_{/\!/}$ decreases with the applied magnetic field H in the range 0-5000 Gauss at 298 K and P = 100 kPa. In different experiments the field H was applied in the directions collinear and perpendicular with respect to the electrical flux, J. However, it is worth to note that no changes in the current were detected when $H \perp J$. Within the time resolution of our set-up (3 seconds), no observable delay was observed between a change of the magnetic field H and the resulting stabilization of the resistance *R*. This stems from the fact that

nanoparticles are small enough to ensure that each one is a single magnetic domain and superparamagnetic with a low T_B (179 K at H=0), leading to fast relaxation kinetics at room temperature.

The dependence of ρ with H and P was fitted by a simple model described in previous work [14]. Essentially, we assume that the intergrain conduction between silver-covered superparamagnetic grains in presence of an external magnetic field H and a pressure P is considered as an equivalent electrical model formed by two resistances in series, referred as R_i and R_H. The total intergrain resistance is then taken equal to (R_i + R_H). Here, R_i represents an intergrain resistance accounting for the electron-jumps between grains in a polycrystalline material which is considered here as dependent of P and independent of H. The resistance R_H accounts for the effect of partially matching the average spins of both grains by spin-alignment through the presence of H (which increases with increasing the magnetization of magnetite within the Fe_3O_4@Ag micro particles). Under these hypotheses, the expression below can be obtained:

$$\rho_k(T,P,H) = A_k(T)\exp\left(-\alpha_k \frac{P}{E_k}\right) + B_k \exp\left(-\frac{\gamma_k H}{KT}\right) \quad (1)$$

where K is Boltzmann's constant, the subscript k stands for the directions ⊥ or || to the needles, $A_k(T)$ is only dependent on the temperature T, E_k represents the Young´s modulus, and B_k, α_k, and γ_k are only dependent on the composition of the MRE (filler concentration). All these parameters can be recovered from the performed experiments (Figure 6). Thus, it was obtained: $\gamma/(K \cdot T) = (2.1\pm0.3)\cdot10^{-3}$ G^{-1}, $A = (13.1\pm0.8)$ Ω·cm, $B = (4.0\pm0.3)$ Ω·cm and $\alpha = 21\pm3$ for PDMS-Fe_3O_4@Ag 5% *w/w* in the direction parallel to the needles (conductive columns).

It should be noted that resistivity curves as a function of the applied pressure are not modified after 10 cycles. Analogously to what happens with the elastic properties of the

material, this can be justified by the absence of Mullins effect [19–21]. The same behavior is observed with the resistivity curves as a function of the applied magnetic field.

3.2.D. Verification of non-transversal conductivity and commutation cycles

Figure 7 shows the absence of significant transversal conductivity for an elastomeric connector of 2 mm thickness. Measurements were performed using the set-up shown in Figure 1.This result was observed also for samples of 1 and 3 mm thickness, which is consistent with the no variation of the resistivities ($\rho_{\perp}$ and $\rho_{/\!/}$) with the sample thickness. Figure 7a1 shows the applied potential between contacts (conducting regions in Figure 1) as a function of time. A trapezoidal potential-time function was used. When the current between vertically matched contacts is measured, for example between C and C' conducting regions (Figure 1), an immediate response is obtained. The induced current profile matched perfectly the profile of the applied voltage, indicating an ohmic behavior (Figure 7b). On the other hand, no measurable current was detected between contacts that do not coincide vertically. These results can be easily interpreted in terms of a very high degree of electrical anisotropy (no electric flow component transverse to the chains of the inorganic material is observed).

4. Conclusions

Silver-covered inorganic material–polymer composites, Fe_3O_4@Ag-PDMS 5% *w/w*, were obtained displaying elastic, magnetic and electrical anisotropic properties. It is worth noting that the observed magneto-/piezoresistive effects were generated using superparamagnetic nanoparticles with low T_B as seeds for the processed materials, resulting not only in composites without magnetic hysteresis, but also with a fast

response (relaxation time) of the resistance R to changes in applied magnetic field H. These remarkable results broaden the spectrum of possibilities when designing devices, as it is demonstrated that it is not indispensable to use ferro- or ferrimagnetic particles for obtaining the desired anisotropic properties, which, in this case, are stabilized by the curing of the PDMS resin. Actually, a high degree of anisotropy was obtained by using fillers that are both highly magnetic and electrical conductors, and loading the polymer with relatively low concentration of fillers (clearly lower than those used by other authors [10,26–28]). The combination of these factors when curing the composites in the presence of a uniform magnetic field is the key for getting final products with anisotropic properties. For instance, the absence of transverse conduction was achieved when preparing composites with 5% *w/w* but transverse conduction was already observed at higher loadings (for instance at 15% *w/w* [14]). Thus, the system allows changing different variables such as the magnetic field during curing and the filler concentration in the range 5-10 %*w/w* which can be optimized for the particular desired application.

The absence of hysteresis in the elastic, piezoresistive and magnetoresistive properties can be associated to the lack of relevant adhesion between the inorganic fillers and the PDMS matrix, manifested by the clear separation at the contact PDMS-fillers (observed by SEM). The fillers and the matrix appear contactless after curing. This separation is possibly the reason why the so-called Mullins effect [19–21] was not observed in the cured structured filler-elastomer composites studied here. The Mullins effect refers to appreciable changes in the physical properties of the composite after the first compression or extension and is attributed to relative displacements between filler and the matrix induced when a strain is applied for the first time. The apparent absence of strong matrix-polymer bonds can be thought to cause the absence of an observable

Mullins effect, thus the lack of particle-matrix adhesion in inorganic-PDMS composites seems to play a favorable role in avoiding hysteresis of the elastic and electric properties as well. Mullins effect are observed mainly in elastomers partly (which is not the case here with PDMS) and filled composites (our case), but the degree is expected to depend on the filler volume fraction and organization, which affects the local mechanical behavior. In our case, the filler organization is strongly dependent on the magnetic field. Of course, more extended experiments such as tensile loading or isostatic pressure measurements would be needed to complete clarify these aspects.

The simple setup implemented in order to measure electric conduction between different points at the bottom and top of the composite film allowed measuring resistances between electrical contacts separated by 1.5 millimeter. Transversal conduction was not observed ($\rho_{\perp} > 62$ MΩ·cm), thus the composite essentially behaves as an insulator in that direction. On the other hand, the longitudinal electrical conduction (parallel to the pseudo-chains) presents ohmic behavior (threshold or rectifier effects were not observed). No electrical hysteresis was detected in the commutation cycles and no phase delays between the detected current and applied voltage was observed within our time resolution scale (about 50 ms). The material behaves as "reversible", which in this context indicates that the response curves of the material to external pressure and / or external magnetic fields (resistivity as function of P and/or H) do not exhibit hysteresis.

The described properties are appropriate for implementing anisotropic strain sensors (using the piezoresistive behavior) or in applications such as integration of pressure-magnetic field sensors or where benefits can be taken from modulating the electrical conduction with a magnetic field (magnetoresistive effect). A key issue for these applications is the highly reproducible electrical response of the prepared composites

after successive cycles of applied external pressure or magnetic field. The presented composites have the additional feature of not being irreversibly magnetized at room temperature, as the material is in the superparamagnetic state. Finally, one of the most promising application is the implementation of the composites as Zebra-like connectors for parallel flip-chip connections with the comparative advantages of allowing to implement 2-D devices (instead of the traditional 3-D connectors) with elastic behavior and displaying both anisotropic magnetoresistance and piezoresistivity that can be used to modulate the conduction between contact points.

Acknowledgments

GJ and RMN are research members of the National Council of Research and Technology (CONICET, Argentina). JLM is an undergraduate fellowship of the University of Buenos Aires (UBA). Financial support was received from the University of Buenos Aires (UBACyT 2008-2010, project X157), CONICET (PIP 6382) and École Polytechnique Fédérale de Lausanne (EPFL, International Cooperation Program). The authors thank the Center of Advanced Microscopy (CMA) at UBA for obtaining the presented images and pictures.

References

[1] J. Wang, M. Scampicchio, R. Laocharoensuk, F. Valentini, O. González-García, J. Burdick, Magnetic tuning of the electrochemical reactivity through controlled surface orientation of catalytic nanowires, Journal of the American Chemical Society. 128 (2006) 4562–4563.

[2] O.T. Mefford, M.R.J. Carroll, M.L. Vadala, J.D. Goff, R. Mejia-Ariza, M. Saunders, et al., Size Analysis of PDMS−Magnetite Nanoparticle Complexes: Experiment and Theory, Chem. Mater. 20 (2008) 2184–2191.

[3] A. Lappas, A. Zorko, E. Wortham, R.N. Das, E.P. Giannelis, P. Cevc, et al., Low-energy magnetic excitations and morphology in layered hybrid perovskite - poly(dimethylsiloxane) nanocomposites, Chemistry of Materials. 17 (2005) 1199–1207.

[4] L. Lanotte, G. Ausanio, C. Hison, V. Iannotti, C. Luponio, The potentiality of composite elastic magnets as novel materials for sensors and actuators, Sensors and Actuators, A: Physical. 106 (2003) 56–60.
[5] M. Farshad, A. Benine, Magnetoactive elastomer composites, Polymer Testing. 23 (2004) 347–353.
[6] Z. Varga, G. Filipcsei, M. Zrínyi, Smart composites with controlled anisotropy, Polymer. 46 (2005) 7779–7787.
[7] Z. Varga, G. Filipcsei, M. Zrínyi, Magnetic field sensitive functional elastomers with tuneable elastic modulus, Polymer. 47 (2006) 227–233.
[8] S.E. Jacobo, J.C. Aphesteguy, R. Lopez Anton, N.N. Schegoleva, G.V. Kurlyandskaya, Influence of the preparation procedure on the properties of polyaniline based magnetic composites, European Polymer Journal. 43 (2007) 1333–1346.
[9] G. Filipcsei, I. Csetneki, A. Szilágyi, M. Zrínyi, Magnetic field-responsive smart polymer composites, Adv. Polym. Sci. 206 (2007) 137–89.
[10] N. Kchit, G. Bossis, Piezoresistivity of magnetorheological elastomers, Journal of Physics Condensed Matter. 20 (2008) 204136-204141.
[11] H. Denver, T. Heiman, E. Martin, A. Gupta, D.-A. Borca-Tasciuc, Fabrication of polydimethylsiloxane composites with nickel nanoparticle and nanowire fillers and study of their mechanical and magnetic properties, Journal of Applied Physics. 106 (2009) 64909-64914.
[12] P. Record, C. Popov, J. Fletcher, E. Abraham, Z. Huang, H. Chang, et al., Direct and converse magnetoelectic effect in laminate bonded Terfenol-D-PZT composites, Sensors and Actuators, B: Chemical. 126 (2007) 344–349.
[13] K. Keshoju, L. Sun, Mechanical characterization of magnetic nanowire-polydimethylsiloxane composites, Journal of Applied Physics. 105 (2009) 23515-23520 .
[14] J.L. Mietta, M.M. Ruiz, P.S. Antonel, O. Perez, A. Butera, G. Jorge, R.Martín Negri, Anisotropic magnetoresistance and piezoresistivity in structured Fe3O4-silver particles in PDMS elastomers at room temperature, Langmuir. 28 (2012), 6985–6996.
[15] P. Soledad Antonel, G. Jorge, O.E. Perez, A. Butera, A. Gabriela Leyva, R. Martín Negri, Magnetic and elastic properties of CoFe2O4- polydimethylsiloxane magnetically oriented elastomer nanocomposites, Journal of Applied Physics. 110 (2011) 043920–043920–8.
[16] R.M. Negri, S.D. Rodriguez, D.L. Bernik, F.V. Molina, A. Pilosof, O. Perez, A model for the dependence of the electrical conductance with the applied stress in insulating-conducting composites, Journal of Applied Physics. 107 (2010) 113703–113714.
[17] P.S. Antonel, R.M. Negri, A.G. Leyva, G.A. Jorge, Anisotropy and relaxation processes of uniaxially oriented CoFe2O4 nanoparticles dispersed in PDMS, Physica B: Condensed Matter. 407 (2012) 3165-3167.
[18] M. Knobel, W.C. Nunes, L.M. Socolovsky, E. De Biasi, J.M. Vargas, J.C. Denardin, Superparamagnetism and Other Magnetic Features in Granular Materials: A Review on Ideal and Real Systems, Journal of Nanoscience and Nanotechnology. 8 (2008) 2836–2857.
[19] E. Coquelle, G. Bossis, D. Szabo, F. Giulieri, Micromechanical analysis of an elastomer filled with particles organized in chain-like structure, Journal of Materials Science. 41 (2006) 5941–5953.

[20] E. Coquelle, G. Bossis, Mullins effect in elastomers filled with particles aligned by a magnetic field, International Journal of Solids and Structures. 43 (2006) 7659–7672.
[21] J. Diani, B. Fayolle, P. Gilormini, A review on the Mullins effect, European Polymer Journal. 45 (2009) 601–612.
[22] D.W. Inglis, A method for reducing pressure-induced deformation in silicone microfluidics, Biomicrofluidics. 4 (2010) 026504–026508.
[23] D.-W. Lee, Y.-S. Choi, A novel pressure sensor with a PDMS diaphragm, Microelectronic Engineering. 85 (2008) 1054–1058.
[24] Q. Cheng, Z. Sun, G.A. Meininger, M. Almasri, Note: Mechanical study of micromachined polydimethylsiloxane elastic microposts, Review of Scientific Instruments. 81 (2010) 106104–106104–3.
[25] J. Tong, C.A. Simmons, Y. Sun, Precision patterning of PDMS membranes and applications, Journal of Micromechanics and Microengineering. 18 (2008) 701-705.
[26] I. Bica, The influence of hydrostatic pressure and transverse magnetic field on the electric conductivity of the magnetorheological elastomers, Journal of Industrial and Engineering Chemistry. 18 (2012) 483–486.
[27] X. Wang, F. Gordaninejad, M. Calgar, Y. Liu, J. Sutrisno, A. Fuchs, Sensing Behavior of Magnetorheological Elastomers, Journal of Mechanical Design. 131 (2009) 91004-91010.
[28] J.E. Martin, R.A. Anderson, J. Odinek, D. Adolf, J. Williamson, Controlling percolation in field-structured particle composites: Observations of giant thermoresistance, piezoresistance, and chemiresistance, Phys. Rev. B. 67 (2003) 94207-94218.

Figure captions

Figure 1. Experimental setup for verification of no-transversal conductivity, where d = 1, 2 or 3 mm and total transversal area is 0.8 cm^2: (a) Lateral view. Zoomed area shows SEM image of the structured PDMS-Fe_3O_4@Ag 5 % *w/w* composite (lateral view of inorganic needles – conducting columns). The scale bar size is 300 μm. (b) Top view. (c) Angle view.

Figure 2. Morphological characterization of PDMS-Fe_3O_4@Ag 5% *w/w* cured structured MRE. Optical photographs: (a) lateral view, (b) top view. SEM images: (c) lateral view, (d) top view of the inorganic chains. "NP-Ag" indicates Fe_3O_4@Ag particles.

Figure 3. Histograms of Fe_3O_4@Ag needle diameters (a) and lengths (b) determined on the basis of the SEM image. (c) The arrow indicates the no-adhesion zone between inorganic filler and polymeric matrix in a SEM top view of a chain.

Figure 4. Magnetic hysteresis curves at 25 °C (a) and ZFC - FC magnetization (M) vs. temperature curves at $H = 0.01$ T (b) for the PDMS-Fe_3O_4@Ag structured composite with filler concentration 5% *w/w*, both in parallel direction respect to the inorganic material needles.

Figure 5. Elasticity results for a 5% *w/w* composite measured in the direction parallel to the needles. (a) Cycles of pressure vs. compression time (t) (speed of compression $v = 100$ μm·s^{-1}; maximum strain: 20%). (b) Relaxation curve: the sample is compressed up to a 20% strain under the same conditions as in (a), and then the compression probe is kept at that strain for 10 s.

Figure 6. (a) Cyclic voltammograms for PDMS-Fe_3O_4@Ag structured composite with filler concentration 5% *w/w* at room temperature. Scan rate is 50 mV·s^{-1}. The arrow shows the increase of the applied pressure. $P1 = 0$ kPa; $P2 = 12$ kPa; $P3 = 39$ kPa; $P4 = 139$ kPa; $P5 = 549$ kPa.
Longitudinal resistivity of PDMS-Fe_3O_4@Ag structured composite with filler concentration 5% *w/w* as a function of applied pressure (b) and magnetic field (c). The solid lines represent the model fit (Eq. 1 with $H = 0$ (a) and $P = 100$ kPa (b)). The transverse resistivity maintained a value higher than 60 MΩ·cm regardless of the pressure and applied field.

Figure 7. (a) Verification of no-transversal conductivity in Figure 1 setup ($d = 2$ mm): (1) Potential between contacts (conducting regions in Figure 1) i and j' as function of time. (2) Current intensity between contacts i and j' as function of time with i = j. (3) Current intensity between contacts i and j' as function of time with i ≠ j. (b) Commutation cycles for $d = 2$ mm. The maximum current intensity corresponds to $V = 2.2$ mV. In all cases i,j = A,B,C,D,E (see Figure 1).

Table 1. Glossary of terms.

PDMS	polydimethylsiloxane
Fe_3O_4@Ag	silver-covered magnetite microparticles
MRE	magnetorheological elastomers
H_{curing}	uniform magnetic field using in curing of MRE
H	magnetic field
XRD	X-ray powder diffraction analysis
SEM	scanning electron microscope
TEM	transmission electron microscope
VSM	Vibrating Sample Magnetometer
ZFC	Zero Field Cooling magnetization curve
FC	Field Cooling magnetization curve
SQUID	Superconducting Quantum Interference Device
d_i	MRE sample thickness in absence of compression
NP	nanoparticles
T	Temperature
T_B	blocking temperature
Φ_v	Filler chains volume fraction in MRE samples
M_S	saturation magnetization
$E_\perp$	Young´s modulus in perpendicular direction respect to the needles
$E_{/\!/}$	Young´s modulus in parallel direction respect to the needles
σ	Electrical conductance
ρ	Electrical resistivity
R	Electrical resistance
P	Pressure
K	Boltzmann's constant

Figure(s)
Click here to download high resolution image

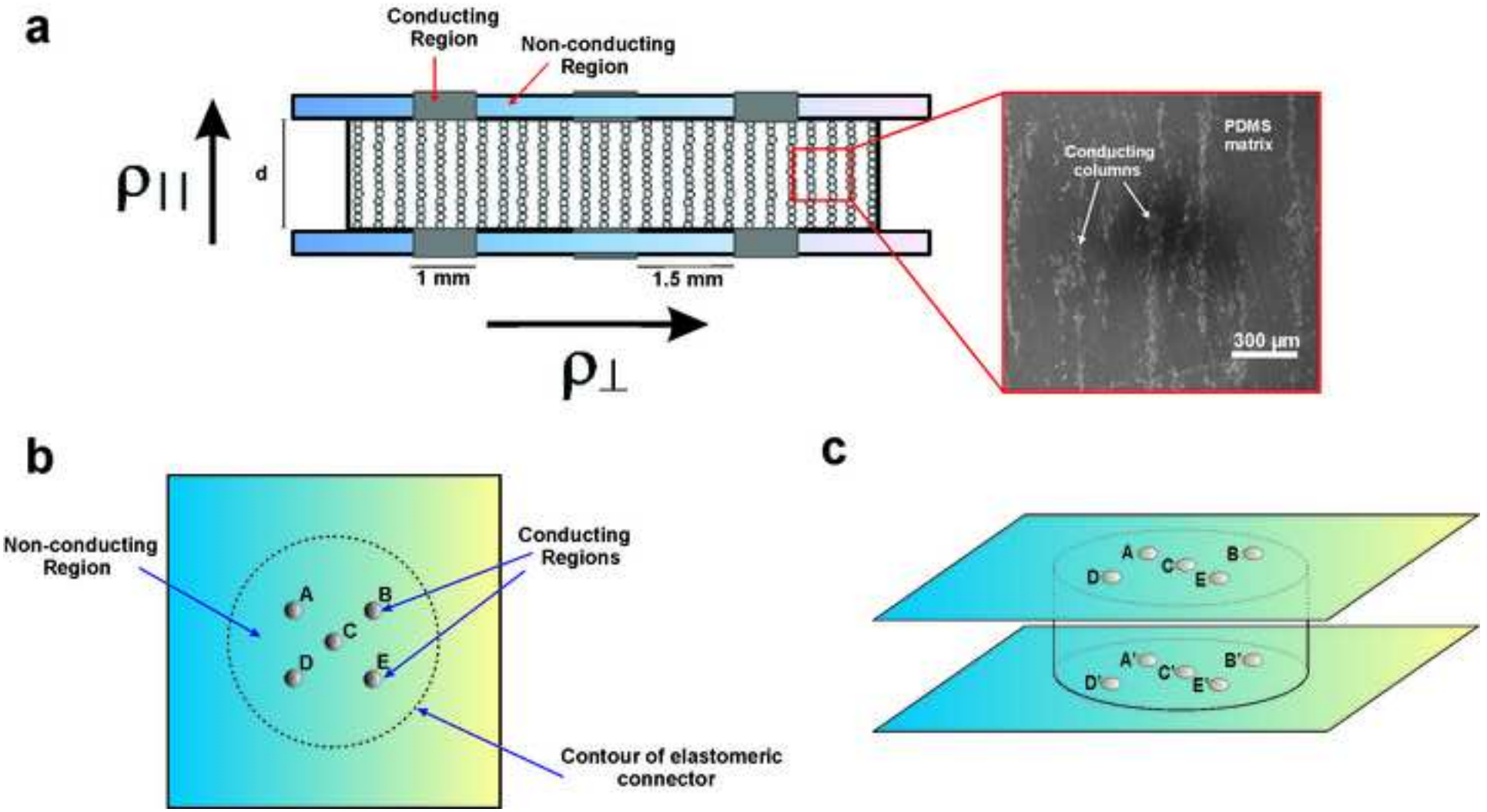

Figure(s)
Click here to download high resolution image

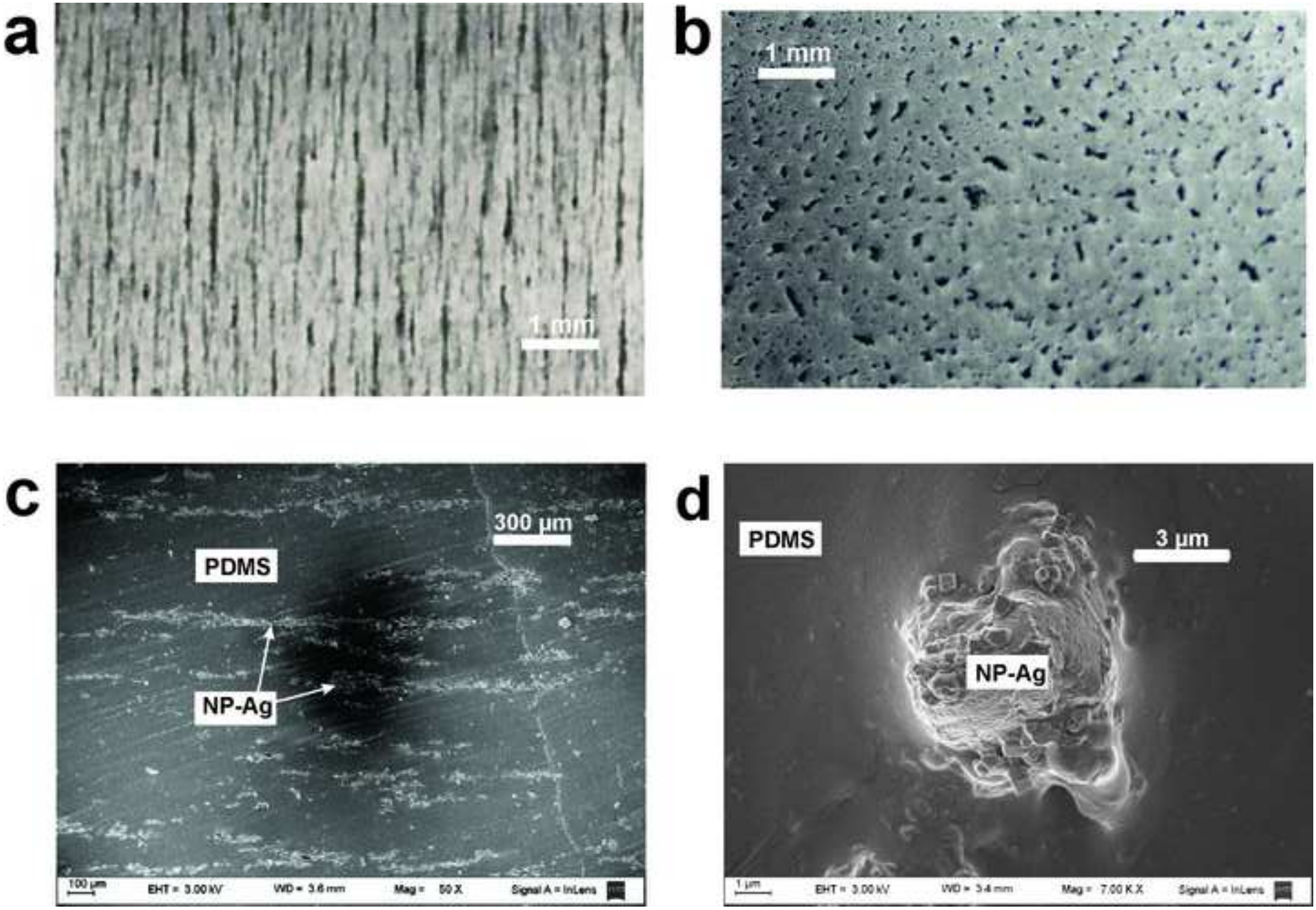

Figure(s)

Click here to download high resolution image

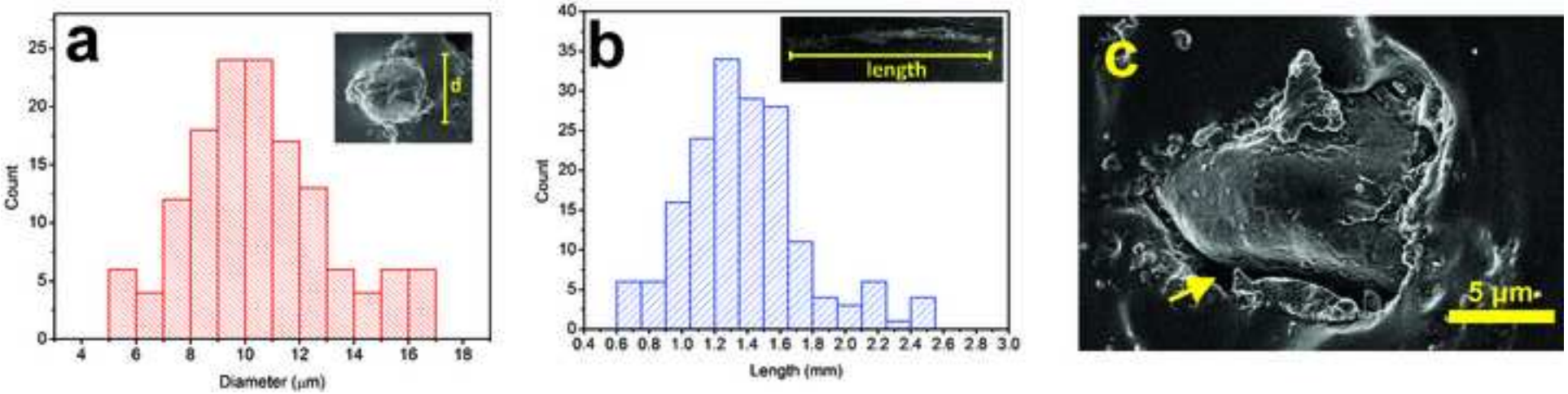

Figure(s)

Click here to download high resolution image

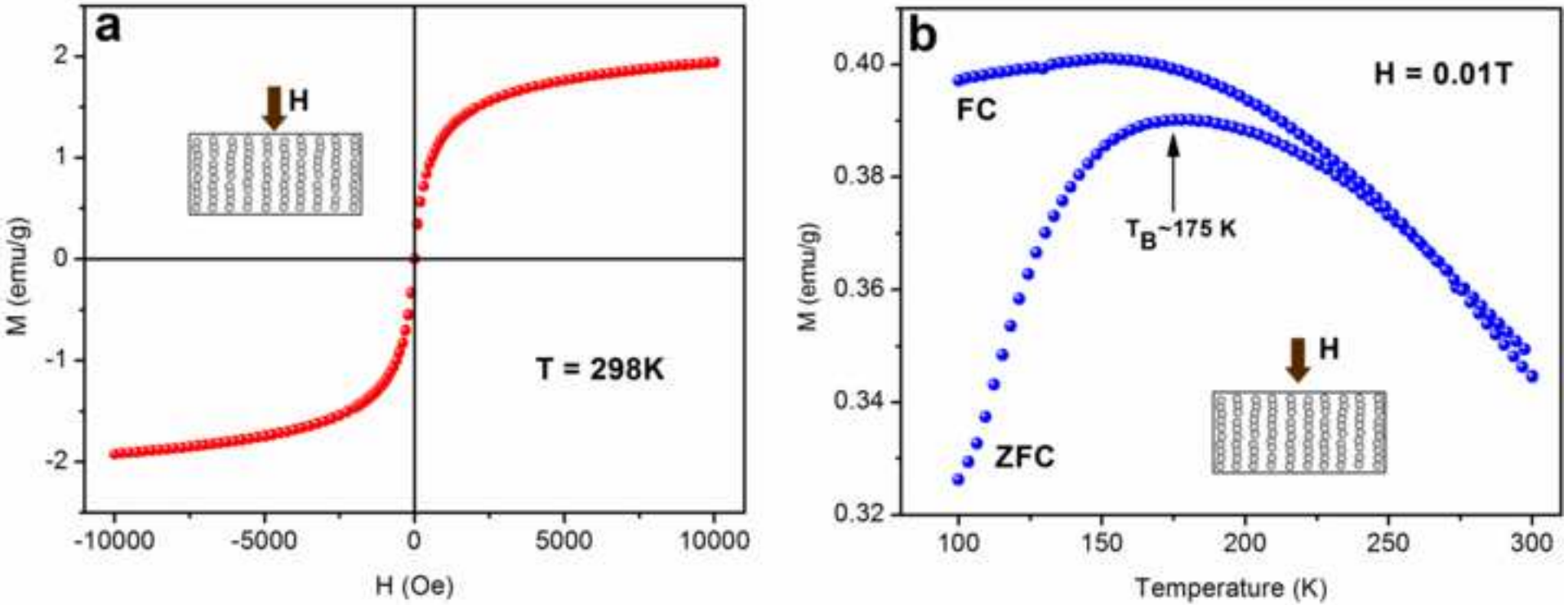

Figure(s)
Click here to download high resolution image

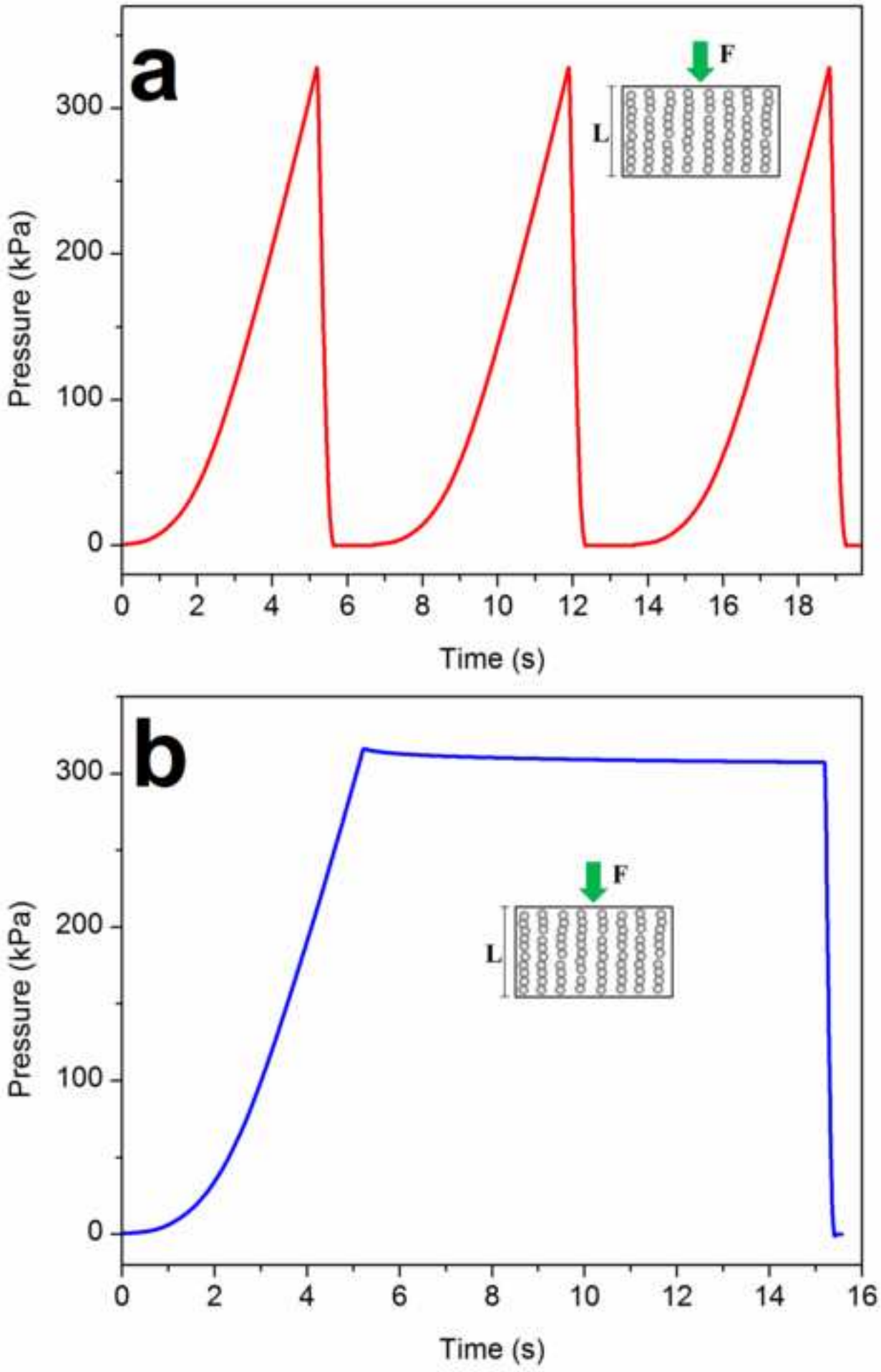

Figure(s)

Click here to download high resolution image

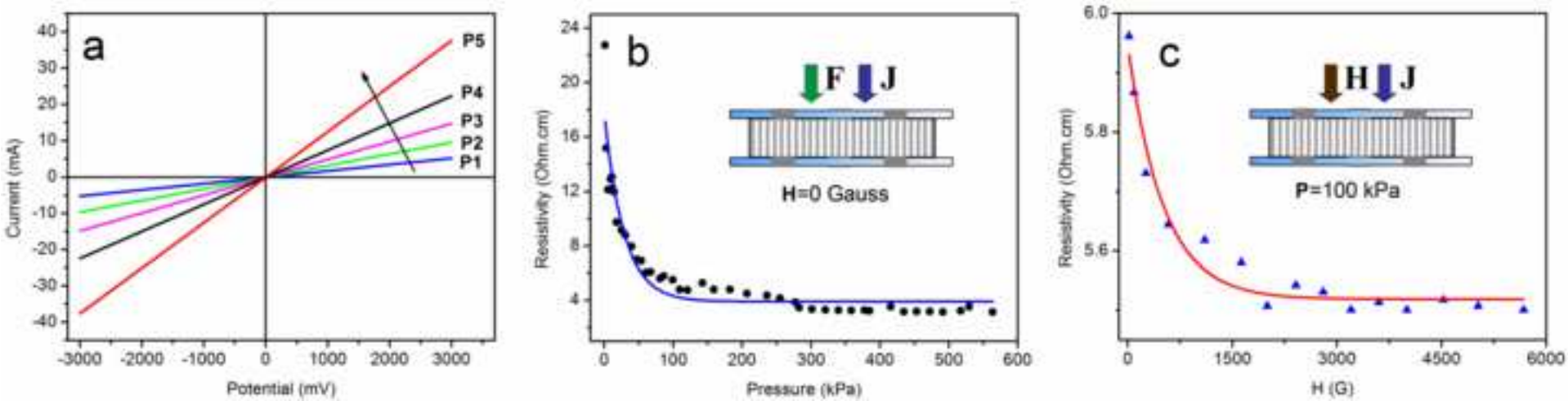

Figure(s)

Click here to download high resolution image

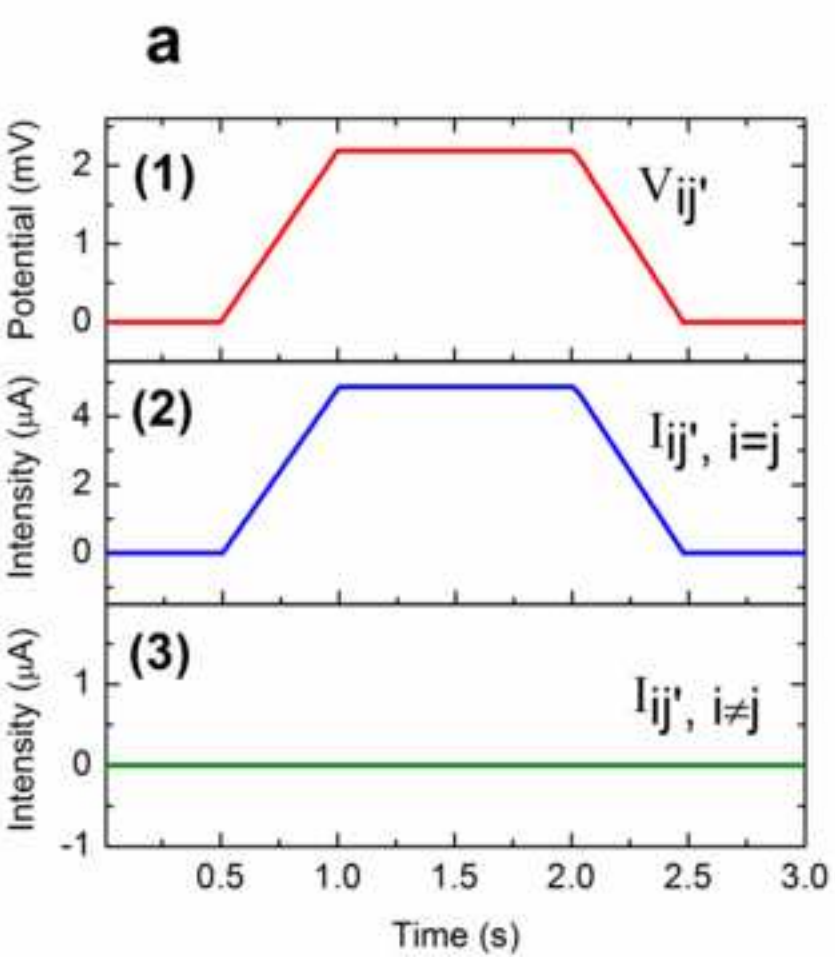

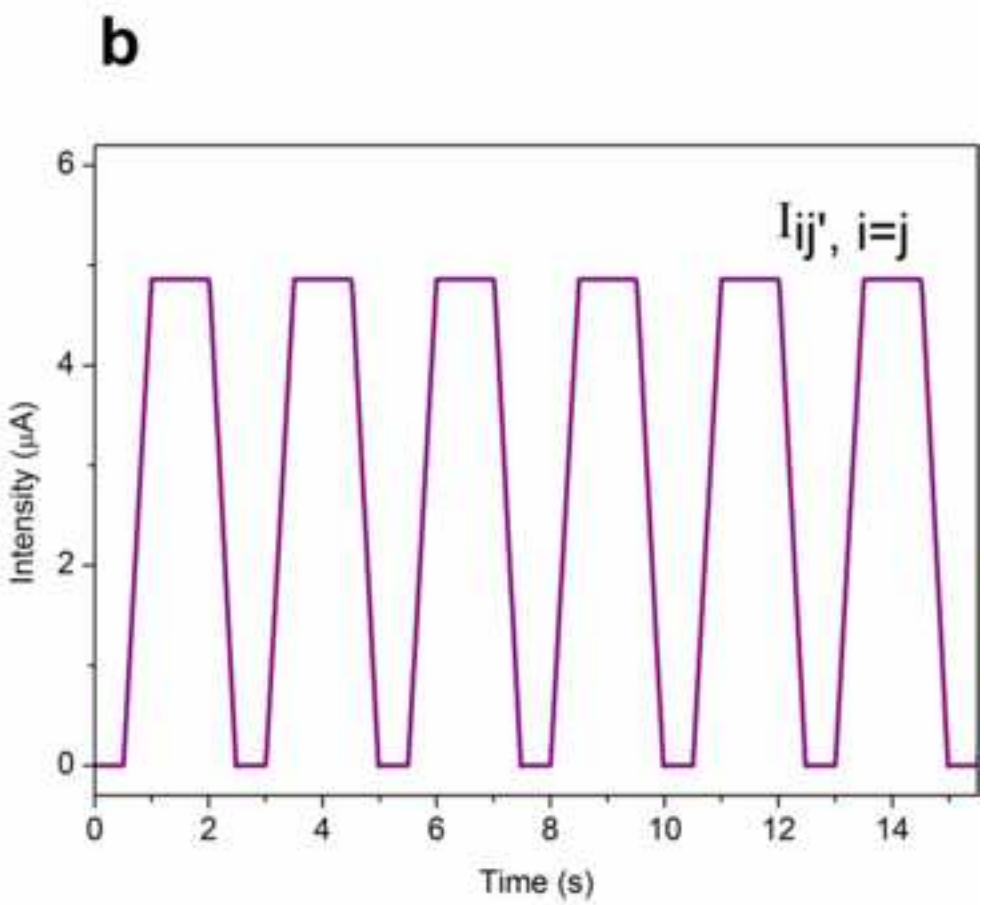

Table(if any)

PDMS	polydimethylsiloxane
Fe_3O_4@Ag	silver-covered magnetite microparticles
MRE	magnetorheological elastomers
H_{curing}	uniform magnetic field using in curing of MRE
H	magnetic field
XRD	X-ray powder diffraction analysis
SEM	scanning electron microscope
TEM	transmission electron microscope
VSM	Vibrating Sample Magnetometer
ZFC	Zero Field Cooling magnetization curve
FC	Field Cooling magnetization curve
SQUID	Superconducting Quantum Interference Device
d_i	MRE sample thickness in absence of compression
NP	nanoparticles
T	Temperature
T_B	blocking temperature
Φ_v	Filler chains volume fraction in MRE samples
M_S	saturation magnetization
$E_\perp$	Young´s modulus in perpendicular direction respect to the needles
$E_{/\!/}$	Young´s modulus in parallel direction respect to the needles
σ	Electrical conductance
ρ	Electrical resistivity
R	Electrical resistance
P	Pressure
K	Boltzmann's constant

*Highlights (for review)

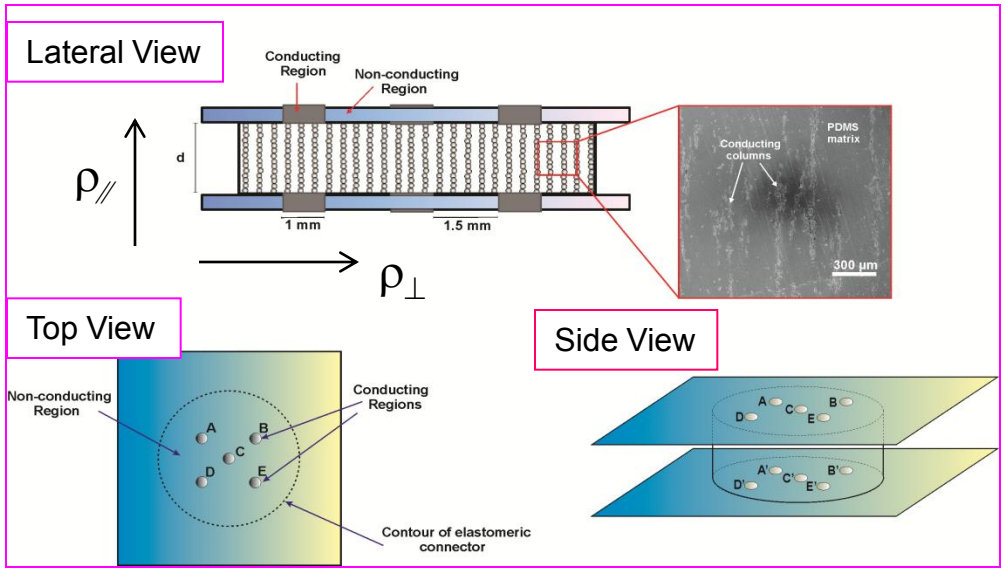

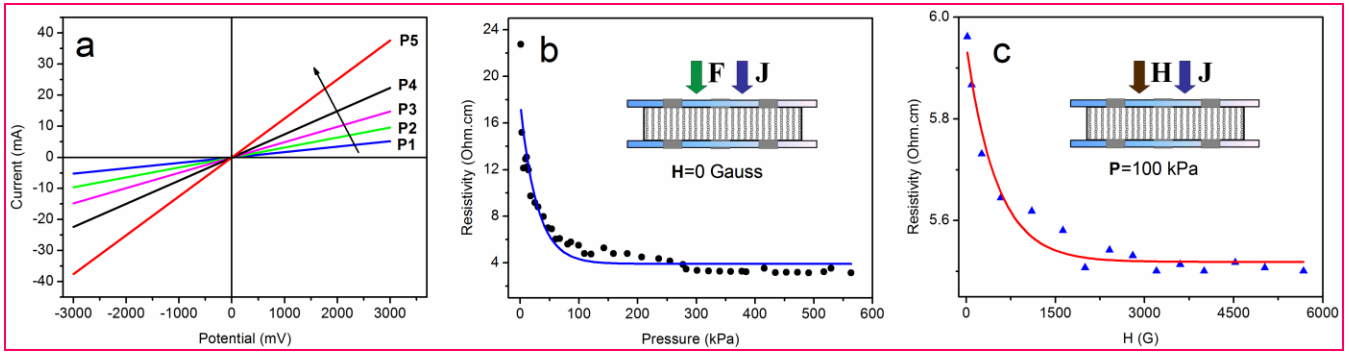

Magnetoelastomer. Anisotropic Magnetoresistance and Piezoelectricity. Unidirectional conduction